# Characterization of a silicon-on-insulator based thin film resistor in electrolyte solutions for sensor applications

M. G. Nikolaides, S. Rauschenbach, and A. R. Bausch[a)]
*Lehrstuhl für Biophysik—E22, Technische Universität München*

(Received 4 August 2003; accepted 5 January 2004)

We characterize the recently introduced silicon-on-insulator based thin film resistor in electrolyte solutions and demonstrate its use as a pH sensing device. The sensor's response function can be tuned by a back gate potential, which is demonstrated by employing known changes of the pH of the solution. The highest sensitivity to pH changes is obtained when the charge carrier concentration at the back interface of the thin Si-film is low compared to the front interface. Calibration measurements with a reference electrode are used to relate the obtained resistance to the surface potential. Applying the site binding model to fit the measured data for variations of the pH gives excellent agreement. The sensors response can be related to a surface potential change of $-50$ mV/pH and from the obtained signal–to–noise ratio, the detection limit can be estimated to be 0.03 pH. For a (bio-)molecular use of the sensor element, a passivation of the silicon oxide surface against this pH response can be achieved by depositing an organic layer of polymethyl-methacrylate (PMMA) onto the devices by spin coating. As expected, the pH response of the surface disappears after the deposition of PMMA. This passivation technique provides an easy and reliable way to obtain a biocompatible interface, which can be further functionalized for the detection of specific molecular recognition events. © *2004 American Institute of Physics.*
[DOI: 10.1063/1.1650880]

## INTRODUCTION

Monitoring the composition of aqueous solutions or detecting specific and unspecific binding of molecules with semiconductor devices is becoming increasingly important.[1–4] Possible applications are ranging from monitoring enzymatic activity in cells to controlling the level of pollution in air and drinking water.[5–7] The most prominent and most extensively studied devices are ion selective field effect transistors (ISFET's), which were introduced by Bergveld.[8] Recently, two-dimensional electron gases in GaAs/AlGaAs heterostructures were introduced as sensor devices.[9] However, the surface of GaAs is highly unstable in aqueous solutions and therefore their applicability as sensors is limited.[10] In contrast, $SiO_2$ is the best studied surface for biocompatible functionalization and also for the detection of pH changes in electrolyte solutions.[11,12] The dissociation of the surface OH-groups of the native $SiO_2$ surface and the concomitant change of the surface potential can be described by the site binding model.[13] Variations of the surface potential evoked by varying salt concentration are well described by the Grahame equation and are very sensitively detected by the recently introduced silicon-on-insulator (SOI) based resistor.[14] The sensor consists of a silicon–silicon oxide layer stack (Si (100) (30 nm)/$SiO_2$ (100 nm)/bulk-Si), as shown in Fig. 1(b). The resistance of the thin silicon sensing layer is measured as the electrolyte on top of the sensor is exchanged.

While the sensitivity of the bare sensor devices toward changes in pH is determined by the density of the reactive Si–OH surface groups, the attenuation and the signal–to–noise ratio is given by the electronic properties of the crystalline silicon sensing layer.[15] Typically, the working point of ISFET's is chosen to be in the saturation region to attenuate surface potential variations the most. The reference electrode in the electrolyte solution is at the same time used to set the working point and as measurement signal in a feedback configuration.

We show that the sensitivity of the SOI based resistor towards surface events is tunable by an applied back gate voltage and in the case of pH changes can be as high as $-50$ mV/pH.

The sensitivity can be tuned using the backside gate to control the carrier concentration in the sensing layer. By adjusting the back gate voltage, the relation between the front and back interface contribution to the overall conductance can be influenced. In the high sensitivity case, the major part of the electrical current flows close to the front side of the silicon sensing layer and is greatly influenced by changes of the surface potential. At the same time, the backside of the thin silicon film is mainly depleted, hence contributing only a minor part to the overall current.

Variations of the surface charge density by means of pH changes in electrolyte solutions are used to demonstrate the tunable attenuation. The thin film resistance is measured in a four terminal geometry and related to the surface potential by calibration measurements using a reference electrode. The data show good agreement with the theoretical site-binding model and the signal–to–noise ratio allows the detection of changes of the pH as small as 0.03.

To passivate the surface against buffer effects for later molecular recognition events and to make the surface bio-

a)Electronic mail: abausch@ph.tum.de

 

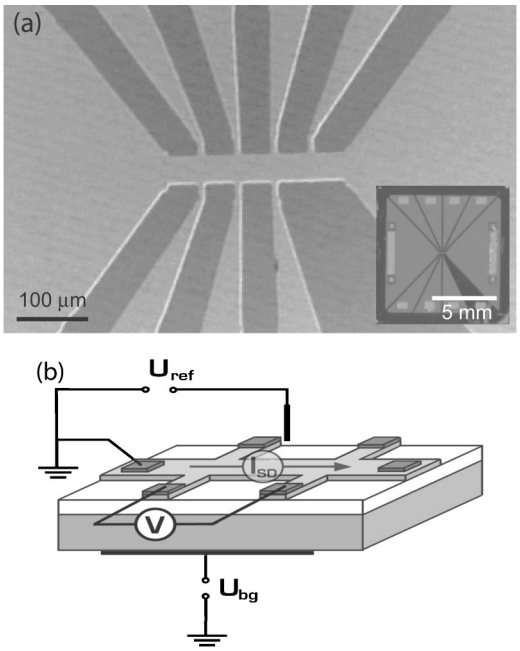


FIG. 1. (a) Optical micrograph of the sensing device. Bright regions indicate conducting silicon, insulating silicon dioxide appears dark. The dimensions of the active hallbar in the middle are 240 $\mu$m$\times$80 $\mu$m. The inset shows the complete chip with the sensing area in the middle and the metal contacts at the outer part of the chip. For the electrolyte measurements, a flow chamber was put on top of the chip limiting the contact of liquids to the active hall bar structure and allowing a rapid exchange of the electrolyte solution at the interface. (b) Sketch of the SOI devices used to measure the changes in surface potential. A constant current was applied between the source and drain contacts of the hall bar. The measured voltage drop between two adjacent contacts directly yields the sheet square resistance. The SOI layer sequence from top to bottom reads: 2–3 nm natural Si oxide (not shown), 30 nm low doped crystalline Si (dark gray, sensing layer), 100 nm buried oxide (light gray), and 675 $\mu$m Si handle wafer (dark gray).

compatible, a thin layer of poly-methyl-methacrylat (PMMA) is spin coated onto the device. As expected, the pH response disappears over the whole range of back gate voltages. This passivation technique provides an easy and reliable way to obtain a biocompatible and hydrophobic surface,[16] which can be further modified to enable the detection of specific binding events.

## MATERIALS AND METHODS

Figure 1(a) shows an optical micrograph of the device used for the experiments with the active hall bar in the middle of the chip and the electrical contacts on the outer part. Figure 1(b) shows a sketch of the measurement setup and the layer structure. The sensor layer has a thickness of 30 nm and was slightly *p*-doped (Boron, $c=10^{16}$ cm$^{-3}$) sitting on top of a 100 nm thick buried oxide layer. This buried oxide isolates the sensor layer electrically from the bulk silicon substrate. The device is covered by the native oxide (2–3 nm thick). The active area consists of a hall bar structure in the middle of the chip with dimensions of 240 $\mu$m $\times$80 $\mu$m. The electrical contacts consist of 50 nm thick aluminum annealed for 2 s at 300 °C.

The resistance of the sensing layer is measured in a four-point measurement to be independent of the contact resistance. A current is applied from source to drain [in Fig. 1(a) left to right] and the voltage drop between two adjacent contacts is measured. The geometry of the hall bar is designed to measure a square of 80$\times$80 $\mu$m$^2$. Current-voltage characteristics of the thin sensor layer are recorded and a linear behavior is observed for source-drain voltages between $-50$ and $+50$ mV. The slope of these current-voltage characteristics is time averaged over 5 min, yielding the square resistance under constant surface and back gate conditions. To control the sensitivity by changing the charge carrier distribution in the sensor layer, the gate voltage ($U_{bg}$) at the back contact of the sensor was varied and the measurement was carried out for every back gate potential. To ensure the electrical isolation of the sensor layer and to verify that the bulk wafer is not contacted by the aluminum, the leakage current was permanently monitored during the sensor measurements. Typical leakage currents for drain currents of 1 $\mu$A were in the order of $10^{-10}$ A.

Prior to the experiments, the relation between the measured square resistance and the surface potential is determined in a calibration measurement, using an Ag/AgCl reference electrode.

For solvent exchange experiments and to isolate the electrical contacts from the electrolyte, a flow chamber is put on top of the device. The details of the fabrication process and the measurement procedure are described elsewhere.[14]

Although the native silicon oxide is known to be unstable in aqueous solutions, the drift of the devices were negligible after 2 h equilibration in electrolyte solutions. To test the stability of the sensor signal, measurements were performed over night and stable signals were obtained even after 12 h.

In order to monitor the pH response of the device, 10 mM Phosphate buffer was used with a constant concentration of 90 mM monovalent KCl. The pH of the buffer was changed by titration with HCl or KOH, respectively.

For the spin coating of the passivation layer, PMMA (P.S.S., Germany, $M_w=31.000$) was dissolved in toluene at a concentration of 1 mg/ml. A drop of this solution was deposited on the device and then spinned for 60 s at 1000 rpm. Unless stated otherwise, all chemicals were purchased from Sigma-Aldrich (Munich, Germany) without further purification. All electrolyte solutions were prepared with deionized ($R>18$ M$\Omega$ cm) water (Millipore, France).

## RESULTS AND DISCUSSION

In a first step, the dependence of the thin film resistance on the applied back gate voltage ($U_{bg}$) was determined. The measurements were carried out while the surface was exposed to air at atmospheric conditions. A variation of the back gate voltage drastically changes the resistance of the thin film resistor as shown in Fig. 2.

The two separated regimes can be attributed to an accumulation of holes (negative back gate potential) and to an accumulation of electrons (positive back gate potential) at the back interface of the sensor layer. In the intermediate regime, for $|U_{bg}|<10$ V, the sensors resistance was high and the resistor showed a nonlinear current voltage characteristic

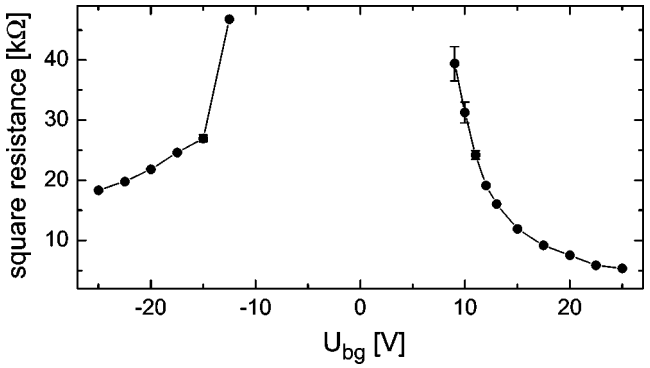


FIG. 2. The resistance of the thin sensing layer depends strongly on the applied back gate voltage. The measurement was done with the front surface of the sensor exposed to air at room temperature. For positive voltages, electrons accumulate at the back interface, whereas for negative voltages, holes are accumulated. Both effects lead to a decrease in resistance. For sensor measurements, a working point was chosen as a compromise between the highest possible sensor signal and a low noise level.

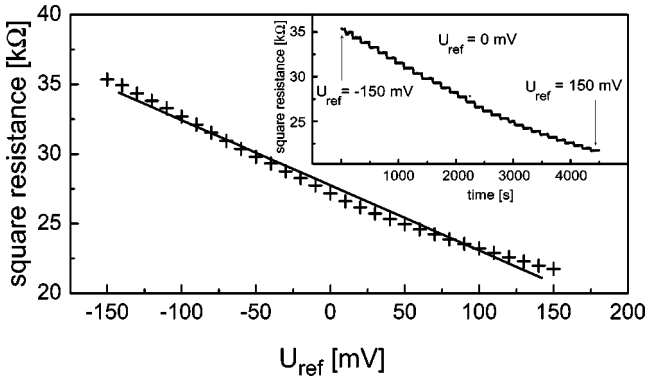


FIG. 3. To relate the measured resistance to surface potential, calibration measurements were carried out using an Ag/AgCl reference electrode. In this example, the potential of the reference electrode was varied between $-150$ and $+150$ mV (at a constant back gate voltage of $+16$ V), yielding an almost linear response of around $-50$ k$\Omega$/V. The inset shows the original data, when the potential of the Ag/AgCl reference electrode is changed in steps of 10 mV.

due to increased noise in the measurement signal.

The screening length in doped semiconductors can be approximated by $L_D=\sqrt{\varepsilon\varepsilon_0 kT/e^2(n+p)}$, with $\varepsilon$ the dielectric constant of the material, $\varepsilon_0$ the vacuum dielectric constant, $e$ the elementary charge and $n$, $p$ the concentration of electrons and holes. This yields 40 nm for $10^{16}$ cm$^{-3}$ doped silicon.[17] The thickness of the silicon sensing layer is in the same order of magnitude. Therefore, potential changes at the front side are screened effectively and thus rather influence the carrier concentration at the front side while potential changes at the backside are mainly influencing the back side carrier concentration.

An increase in sensitivity can be reached, when the back side carrier concentration of the sensing layer is low compared with the front side. In this regime, the contribution of the back interface to the overall conductivity is very small compared to the front interface contribution. Thus, small changes of the surface potential, influencing mainly the front interface, have a great effect on the overall conductivity and therefore result in a strong measurement signal.

For the application as sensor, we choose $+16$ V as the working point. A positive back gate voltage was chosen, as this prevents cations from diffusion into the substrate.[18] A linear response of the sensor was achieved at this voltage, even after the exposure of the surface to electrolyte solutions.

Prior to the sensor experiments, a calibration measurement was performed in order to relate the measured sheet resistance to the surface potential at the oxide/electrolyte interface. An Ag/AgCl reference electrode in the electrolyte solution was used to control the potential at the oxide/electrolyte interface at a constant back gate voltage. The voltage of the reference electrode was varied in a steplike function and the resulting resistance was determined. In Fig. 3, a typical dependence of the resistance from the reference electrode is shown for a constant back gate voltage of $+16$ V. In this regime, the sensors response towards surface potential changes was almost linear with slope $-50$ k$\Omega$/V.

The possibility to tune the sensitivity by the back gate is one of the key properties of the presented SOI resistor for its variable applicability as sensing device. To demonstrate the tunability, a constant jump in pH (pH 2 to pH 7) was detected with the sensor for different back gate voltages. The relation between sheet resistance and back gate voltage after exposure to an electrolyte solution (inset Fig. 4) is similar as under air (Fig. 2), but is shifted to higher resistance values.

Figure 4 shows the detected jump $\Delta R$ in resistance as a function of the back gate voltage between $+16$ and $+30$ V. The detected resistance jump $\Delta R$ of the sensor layer decreases for increasing back gate voltage. The response signal varies by a factor of 4 for the range of applied voltages. This is attributed to the fact that higher back gate voltages induce more charge carriers at the back interface of the sensor layer with the buried oxide. As typical screening lengths are the same order of magnitude like the layer thickness of 30 nm, the back interface is less influenced by changes of the surface potential. Therefore, for high carrier concentrations at the back interface, the relative contribution of the front interface to the overall conductance is smaller. Hence, changes of the

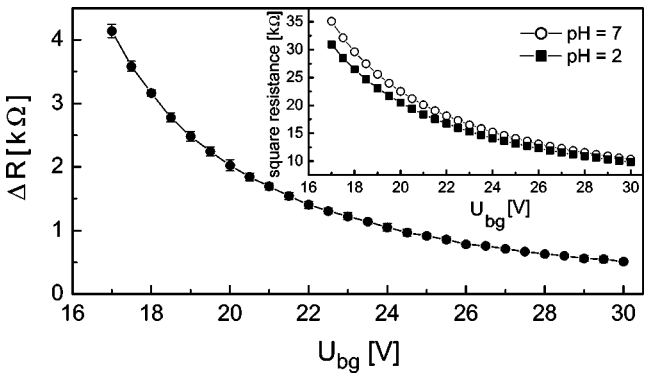


FIG. 4. The response of the sensor toward surface events strongly decreases with increasing carrier concentration at the back interface. In this figure, the resistance jump for a change from pH 2 to pH 7 was measured for different back gate voltages. By applying higher back gate voltages, the carrier concentration at the back interface is increased. Therefore, the ratio of the front interface at the total conductivity is smaller. As mainly the front interface of the sensor layer is influenced by surface events, the sensitivity decreases with increasing back gate voltage.

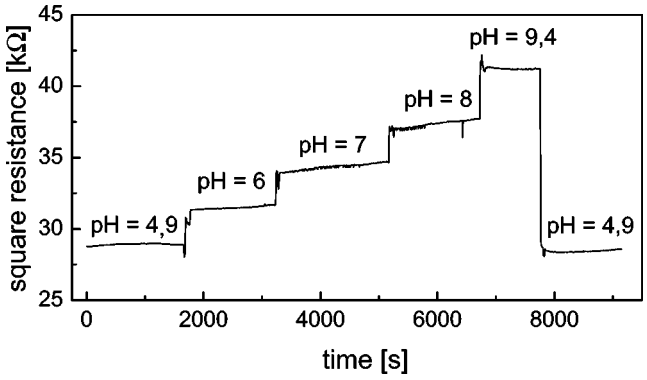


FIG. 5. Measurement of the pH response of the sensor at a constant back gate voltage of +16 V. The resistance immediately followed a pH change of the electrolyte solution on top of the sensor. Going back to the initial value of pH 5, the sensor signal returns to its original level. The response of the device corresponds to 2.6 kΩ/pH and can be related with the help of the calibration measurements to a surface potential change of around −50 mV/pH.

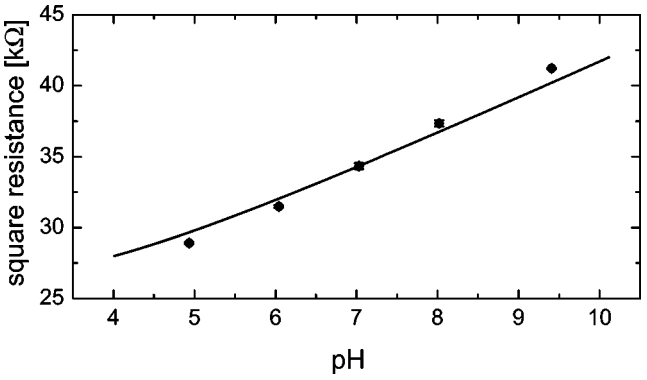


FIG. 6. Comparison of the measured data with the theoretical predictions by the site-binding model. The measured response (black dots) agrees very well with the theoretical predictions from the site-binding theory (solid line). The theoretical curve corresponds to a value of $\beta = 0.15$, in good agreement with literature values and does not include any additional fitting parameter.

surface potential also contribute less to the overall conductance and the sensitivity is smaller. Conversely, at small carrier concentrations, the surface potential induced charge carriers have a relatively high effect. In principle, it would therefore be most desirable to have as few charge carriers as possible. However, the higher the resistance, the smaller the DC signals one has to measure and the higher the disturbance of this signal by undesired noise will be. Therefore, an intermediate value has to be chosen to combine these two requirements.

After the working point is set for every device (in the measurements shown here $U_{bg} = +16$ V), the dependence of the devices toward variations of the pH can be measured at a constant back gate voltage. To ensure turbulent flow conditions for a rapid and complete exchange of the solvents, a microfluidic chamber out of polycarbonate was put on top of the devices. The resistance of the crystalline silicon sensor layer is constantly measured during the exchange of the electrolyte. Figure 5 shows the measured resistance for a pH variation between 5 and 9. The response was fitted linear and each step in pH resulted in a instantaneous change of the square resistance of about 2.6 kΩ. Taking the relation of the square resistance and the surface potential of $-50$ kΩ/V as obtained from the calibration measurements, a pH step of one unit corresponds to a variation of the surface potential of $-52$ mV. Although some papers report similar close Nernstian responses,[19] this value is higher than pH responses of $SiO_2$ surfaces reported in many publications of 30–40 mV/pH.[12] This is attributed to different oxide qualities and different densities of OH surface groups on the different surfaces.

The pH response of $SiO_2$ surfaces is caused by the protonation and deprotonation of the Si–OH surface groups present at the electrolyte/native oxide interface and can be calculated in the site binding model.[20] After the site binding model, the expected pH response of a $SiO_2$ surface is given by

$$2.303(\mathrm{pH}_{\mathrm{pzc}} - \mathrm{pH}) = \frac{q\psi_s}{kT} + \operatorname{arsinh}\left(\frac{q\psi_s}{kT}\frac{1}{\beta}\right).$$

Here, $\mathrm{pH}_{\mathrm{pzc}} = 2.2$ is the point of zero charge, $k$ is Boltzmann's constant, $T$ the temperature, and $\psi_s$ the surface potential. The parameter $\beta$ is $\beta = 2q^2 N_s (K_a K_b)^{1/2}/kTC_{\mathrm{DL}}$, with $K_a$ and $K_b$ being the two chemical equilibrium constants of the oxide surface, $N_s$ the density of surface OH groups and $C_{\mathrm{DL}}$ the double layer capacity.[20] A comparison of our data with the side binding model shows very good agreement (Fig. 6). In the theoretical line shown, the parameter $\beta = 0.15$, which is in excellent agreement with other studies using standard ISFET devices.

The observed noise in the signal of the devices is typically 50–100 Ω. Assuming this value as detection limit and taking the response of 2.6 kΩ per pH step, a detection of variations in pH of 0.03 units would be possible with the device.

In order to increase the sensitivity when the device is used as (bio-) molecular sensor, the surface needs to be passivated against its pH response. To avoid the pH-sensitivity of inorganic insulating films such as $SiO_2$ or $TiO_2$, an organic surface coating can be used. In addition to pH passivation, a hydrophobic layer also represents a biocompatible interface for a further functionalization.[16]

We deposited a layer of PMMA on top of the native oxide by the spin coating technique. At a concentration of 1 mg/ml and a deposition speed of 1000 rpm, a dense layer of PMMA was obtained. The thickness was determined by ellipsometry to be 25 nm. Upon deposition, the contact angle changed from 10° on the clean $SiO_2$ surface to 60° on the PMMA coated device, indicating the hydrophobicity of the PMMA layer. This already indicates that the pH response should be modified, because the chemical properties of the interface are changed. Figure 7 shows the resulting response of the PMMA covered sensor to a pH step from pH 2 to pH 7 for back gate voltages between +21 and +34 V. The deposition of the PMMA suppresses the pH response. At a back gate voltage of +21 V, the normalized change in resistance is reduced from 0.08 to 0.02. If the PMMA layer was

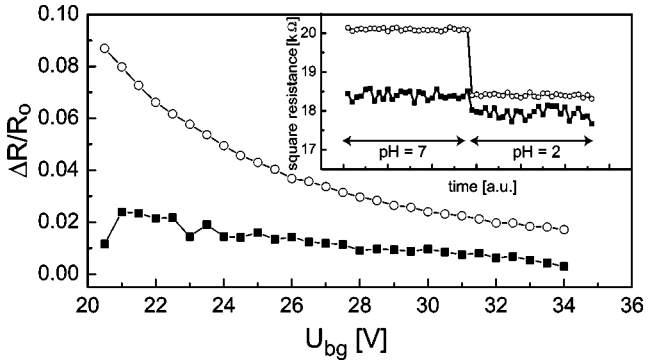


FIG. 7. Relative resistance change between pH=2 and pH=7 for back gate voltages between +21 and +34 V. The open circles correspond to the bare silicon oxide, the closed squares to the PMMA covered device. As can be seen, the pH response is greatly reduced in the case of a PMMA coating. For +21 V, the relative response is reduced from 0.08 to 0.02. The inset shows the response of the device after solvent exchange for an applied back gate of +21 V.

removed by rinsing the sensor with acetone, the original pH response of the device was recovered (Fig. 7).

## CONCLUSION

In conclusion we have shown that SOI based sensor can be used to detect changes of the surface potential with very high sensitivity. The electrical isolation of the sensor layer from the back gate gives the important possibility to tune the sensitivity, which will be useful for the application of the device to different detection schemes. The attenuation of the SOI resistor enables the detection of changes of 0.03 pH. In addition, an easy and reliable way to passivate the surface by spin coating PMMA was demonstrated. This PMMA layer inhibits the $SiO_2$ specific pH response and renders the surface hydrophobic, which can be used for further biofunctionalization.[16] Thus, it comprises the possibility to be used for the construction of a molecular sensor for specific binding of biomolecules.

Both achievements, the tunable sensitivity and the presented passivation technique make the SOI thin film resistor sensor a promising device for the detection of specific biomolecular interactions.

## ACKNOWLEDGMENTS

The authors thank E. Sackmann and G. Abstreiter for many fruitful discussions, and F. Rehfeldt and M. Tanaka for help with the PMMA spin coating. The project was funded within the SFB 563 TP B12. The support of the ''Fonds der Chemie'' is gratefully acknowledged. M.G.N. was supported by the ''Studienstiftung des deutschen Volkes.''

[1] P. Bergveld, Sens. Actuators B **88**, 1 (2003).
[2] Y. Ciu, Q. Wei, H. Park, and C. M. Lieber, Science **293**, 1289 (2001).
[3] G. D. Wu, D. Cahen, P. Graf, R. Naaman, A. Nitzan, and D. Shvarts, Chem. Eur. J. **7**, 1743 (2001).
[4] J. Fritz, E. B. Cooper, S. Gaudet, P. K. Sorger, and S. R. Manalis, Proc. Natl. Acad. Sci. U.S.A. **99**, 14 142 (2002).
[5] J. Brunet, L. Talazac, V. Battut, A. Pauly, J. P. Blanc, J. P. Germain, S. Pellier, and C. Soulier, Thin Solid Films **391**, 308 (2001).
[6] M. J. Schoning and H. Luth, Phys. Status Solidi A **185**, 65 (2001).
[7] A. Fanigliulo, P. Accossato, M. Adami, M. Lanzi, S. Martinoia, S. Paddeu, M. T. Marodi, A. Rossi, M. Sartore, M. Grattarola, and C. Nicolini, Sens. Actuators B **32**, 41 (1996).
[8] P. Bergveld, IEEE Trans. Biomed. Eng. **BM17**, 70 (1970).
[9] K. Gartsman, D. Cahen, A. Kadyshevitch, J. Libman, T. Moav, R. Naaman, A. Shanzer, V. Umansky, and A. Vilan, Chem. Phys. Lett. **283**, 301 (1998).
[10] K. Adlkofer, M. Tanaka, H. Hillebrandt, G. Wiegand, E. Sackmann, T. Bolom, R. Deutschmann, and G. Abstreiter, Appl. Phys. Lett. **76**, 3313 (2000).
[11] G. Elender, M. Kuhner, and E. Sackmann, Biosens. Bioelectron. **11**, 565–577 (1996).
[12] L. Bousse, N. F. Derooij, and P. Bergveld, IEEE Trans. Electron Devices **30**, 1263 (1983).
[13] R. E. G. vanHal, J. C. T. Eijkel, and P. Bergveld, Adv. Colloid Interface Sci. **69**, 31 (1996).
[14] M. G. Nikolaides, S. Rauschenbach, S. Luber, K. Buchholz, M. Tornow, G. Abstreiter, and A. R. Bausch, Chem. Phys. Chem **4**, 1104 (2003).
[15] P. Chattopadhyay, Semicond. Sci. Technol. **13**, 1036–1041 (1998).
[16] E. Sackmann and M. Tanaka, Trends Biotechnol. **18**, 58–64 (2000).
[17] W. Mönch, *Semiconductor Surfaces and Interfaces* (Springer, Berlin, 2001).
[18] M. Rentschler and P. Fromherz, Langmuir **14**, 547–551 (1998).
[19] W. M. Siu and R. S. C. Cobbold, IEEE Trans. Electron Devices **26**, 1805–1815 (1979).
[20] P. Bergveld and A. Sibbald, *Analytical and Biomedical Application of Ion-Selective-Field-Effect Transistors*, Vol. XXIII (Elsevier, Amsterdam 1988).